Supporting Information

K-Mediated Peripheral Electronic Tuning of Low-valence Au Single Atoms for Efficient Acetylene Hydrochlorination

Zhenbang Liu [a], Xiaohui Liu [a], Yawei Geng [a], Xiangfa Meng [a], Sen Wang [a], Yanzhao Dong [a*], Yunsheng Dai [b*], Jinli Zhang [a, c], and Haiyang Zhang [a*]

[a] *School of Chemistry and Chemical Engineering/ State Key Laboratory Incubation Base for Green Processing of Chemical Engineering, Shihezi University, Shihezi, Xinjiang, 832000, P.R. China;*

[b] *Yunnan Precious Metals Lab Co., Ltd., Kunming 650106, China.*

[c] *School of Chemical Engineering and Technology, Tianjin University, Jinnan District, Tianjin, 300072, P.R. China.*

[*] Corresponding authors.

Fax: +86-993-2057006; Tel: +86-993-2057006;

E-mail address: dongyanzhao2012@163.com (Y. Dong); daiysh@ipm.com.cn (Y. Dai); zhy198722@163.com (H. Zhang);

Experiment

S–1 Catalyst preparation

Preparation of K-NC

The support was treated via high-temperature pyrolysis. Specifically, 4 g of dicyandiamide (NH_2CN) and 5.95 g of potassium bromide (KBr) were dissolved in an ethanol/water mixed solvent (V/V=1:1), followed by the addition of 10 g of activated carbon (AC) and stirring for 6 hours. After vacuum drying at 60℃, the mixture was calcined at 560℃ for 4 hours under a N_2 atmosphere (heating rate: 2.2 ℃/min). The K–N co-doped support (K-NC) was obtained after washing and drying.

Preparation of NC

4 g of dicyandiamide (NH_2CN) were dissolved in an ethanol/water mixed solvent (V/V=1:1), followed by the addition of 10 g of activated carbon (AC) and stirring for 6 hours. After vacuum drying at 60℃, the mixture was calcined at 560℃ for 4 hours under a N_2 atmosphere (heating rate: 2.2 ℃/min). The N-doped support (NC) was obtained after washing and drying.

Preparation of Au/K-NC-SA

The catalyst was prepared via the coordination anchoring synthesis strategy. 5 g of

K-NC support was dispersed in deionized water, and 15.59 mL of $HAuCl_4$ solution (10 mg/mL) was slowly added dropwise to it. After bubbling with nitrogen for 30 minutes, the mixture was stirred at 60°C for 6 hours. Following centrifugation and washing, it was vacuum-dried at 60°C. The sample obtained after etching with 1 mol/L HCl solution and subsequent drying was denoted as Au/K-NC-SA.

Preparation of Au/NC-SA

5 g of NC support was dispersed in deionized water, and 15.59 mL of $HAuCl_4$ solution (10 mg/mL) was slowly added dropwise to it. After bubbling with nitrogen for 30 minutes, the mixture was stirred at 60°C for 6 hours. Following centrifugation and washing, it was vacuum-dried at 60°C. The sample obtained after etching with 1 mol/L HCl solution and subsequent drying was denoted as Au/NC-SA.

Preparation of Au/K-NC

The catalyst was prepared via the simple impregnation method with an Au loading of 0.8 wt%. Briefly, 9.6 mL of $HAuCl_4$ solution (10 mg/mL) was added to 20 mL of deionized water. After stirring for 30 minutes until homogeneous, 5 g of K-NC was added. Following 12 hours of stirring, the mixture was refluxed at 70°C for 24 hours. The mixture was vacuum-dried at 70°C for 12 hours, and the resulting sample was denoted as Au/K-NC.

S–2 Catalyst characterization

Raman spectra of the samples were collected using a Renishaw inVia Raman spectrometer. X–ray photoelectron spectroscopy (XPS) analysis was performed on an ESCALAB 250 Xi spectrometer with Al–Kα radiation to obtain the elemental composition and relative contents of the catalysts. Thermogravimetric (TG) data of the catalyst samples were acquired using a NETZSCH STA 449 F5 Jupiter thermogravimetric analyzer. The Brunauer–Emmett–Teller (BET) surface area of the samples was measured via an ASAP 2020C physical adsorption-desorption analyzer. X–ray diffraction (XRD) patterns were obtained using a Bruker D8 Advance X–ray diffractometer with a Cu–Kα radiation source. Temperature–programmed reduction (TPR) was conducted on a Quantachrome AutoChem BET TPR/TPD multifunctional chemisorption analyzer in the temperature range of 25–900°C, under an H_2/Ar

atmosphere (10% H_2) with a heating rate of 10°C·min^{-1}. Temperature–programmed desorption (TPD) was performed on the same Quantachrome AutoChem BET TPR/TPD analyzer in the temperature range of 25–900°C, under an N_2 atmosphere with a heating rate of 10°C·min^{-1}. Transmission electron microscopy (TEM) images and corresponding EDS mappings were obtained using a JEOL JEM 2010 transmission electron microscope. The Au loading in the catalysts was determined by inductively coupled plasma optical emission spectrometry (ICP–OES, Agilent 5110). Aberration-corrected high-angle annular dark-field scanning transmission electron microscopy (AC–HAADF–STEM) measurements of the catalyst samples were carried out using a JEOL JEM–ARM200F aberration-corrected transmission electron microscope. Synchrotron radiation analysis was performed at the BL14W beamline of the Shanghai Synchrotron Radiation Facility (SSRF), where X–ray absorption near edge structure (XANES) and extended X–ray absorption fine structure (EXAFS) data at the Au L_3–edge were collected. Data reduction, data analysis, and EXAFS fitting were performed and analyzed with the Athena and Artemis programs of the Demeter data analysis packages[1] that utilizes the FEFF6 program[2] to fit the EXAFS data. For the X–ray absorption near edge structure (XANES), experimental absorption coefficients as a function of energy, μ(E), were subjected to background subtraction and normalization procedures. The results were reported as "normalized absorption" for all tested samples. The extended X–ray absorption fine structure (EXAFS) data of the prepared catalysts were analyzed using Fourier transform (FT) to determine the coordination structure, including the number, type, and distances of coordination atoms. For Wavelet Transform analysis, the χ(k) exported from Athena was imported into the Hama Fortran code. The parameters were listed as follow: R range, 0–6 Å, k range, 0–12.0 Å^{-1}; k weight, 3; and Morlet function with κ=10, σ=1 was used as the mother wavelet to provide the overall distribution[3].

S–3 Catalyst tests

Catalytic activity evaluation was conducted in a fixed-bed microreactor (inner diameter: 10 mm) coupled with an online detection system (online gas chromatograph, GC). For the experiment, 1 mL of catalyst was loaded into the reactor tube. The

reactor tube was purged with N_2 and heated to 160°C to remove moisture and impurities in the tube and the catalyst. Subsequently, hydrogen chloride (HCl) was introduced to activate the catalyst for 30 minutes. After activation, acetylene (C_2H_2) was fed into the reactor, and the temperature was raised to 180°C to initiate the reaction. Throughout the reaction, the temperature was maintained at 180°C, the feed volume ratio of HCl to C_2H_2 was 1.15, and the acetylene gas hourly space velocity (GHSV(C_2H_2)) was kept at 1200 h^{-1}. The effluent gas passed through an absorption bottle and a drying tube to remove unreacted HCl, and then entered the online GC for product analysis.

Three key indicators, namely acetylene conversion (X_a), vinyl chloride selectivity (S_{VCM}), and reaction rate (r, $kg_{VCM}\cdot kg_{Au}^{-1}\cdot h^{-1}$), were used to comprehensively evaluate the catalytic performance of the catalysts. They are defined and expressed as the following formulas respectively:

$$X_A = 1 - \frac{\Phi_V}{\Phi_0} \times 100\%$$

$$S_{VCM} = \frac{\Phi_{VCM}}{1 - \Phi_V} \times 100\%$$

Wherein, Φ_0 and Φ_v represent the volume fractions of acetylene in the feed gas and the effluent gas after reaction, respectively; Φ_{VCM} denotes the volume fraction of vinyl chloride in the product mixture.

$$r = \frac{F_{C_2H_2} \times 60 \times X_A \times S_{VCM} \times M_{VCM}}{22400 \times W_{Catal.} \times \omega_{Au}}$$

Wherein, F_{C2H2} represents the gas flow rate of C_2H_2 (mL min^{-1}), M_{VCM} denotes the relative molecular mass of vinyl chloride (VCM), $W_{Catal.}$ stands for the mass of the catalyst (g), and ω_{Au} indicates the Au loading in the catalyst (wt.%).

S–4 Computational Methods

All the first-principles spin-polarized calculations were performed by using plane-wave density functional theory (DFT) as implemented in the Vienna Ab Initio Simulation Package (VASP)[4, 5]. The exchange-correlation potential is treated with the Perdew–Burke–Ernzerhof (PBE) formula by using the projected augmented wave

(PAW) method within the generalized gradient approximation (GGA)[6-8]. To describe the ionic cores and take valence electrons into account using a plane wave basis set with a kinetic energy cutoff of 500 eV[9, 10]. Partial occupancies of the Kohn–Sham orbitals were allowed using the Gaussian smearing method and a width of 0.05 eV. The electronic energy was considered self-consistent when the energy change was smaller than 10^{-4} eV. A geometry optimization was considered convergent when the energy change was smaller than 0.06 eV $Å^{-1}$. The Au single-atom catalyst model was constructed based on a 7×7 graphene supercell in the x–y plane, with a vacuum layer of 20 Å along the z–direction to minimize interlayer interactions. The Brillouin zone integral uses the surfaces structures of 3×3×1 K-point sampling for structure. For electronic structure calculations, a finer 7×7×1 K-point grid was adopted. van der Waals interactions were accounted for using Grimme's DFT–D3 method[11], which has been demonstrated to accurately describe both chemical and physical adsorption behaviors in layered material systems. Kinetic barriers are obtained using climbing-image nudged elastic band (CI–NEB)[12, 13]. Five (3) images are interpolated between the initial (IS) and the final state (FS) to acquire minimum energy path (MEP), and geometry of the transition state (TS). The total energy and force thresholds for geometry optimizations are 1×10^{-5} eV and 0.05 eV $Å^{-1}$, respectively. TSs are determined through frequency analysis to ensure only one imaginary frequency existed, assigned to MEP's unstable mode.

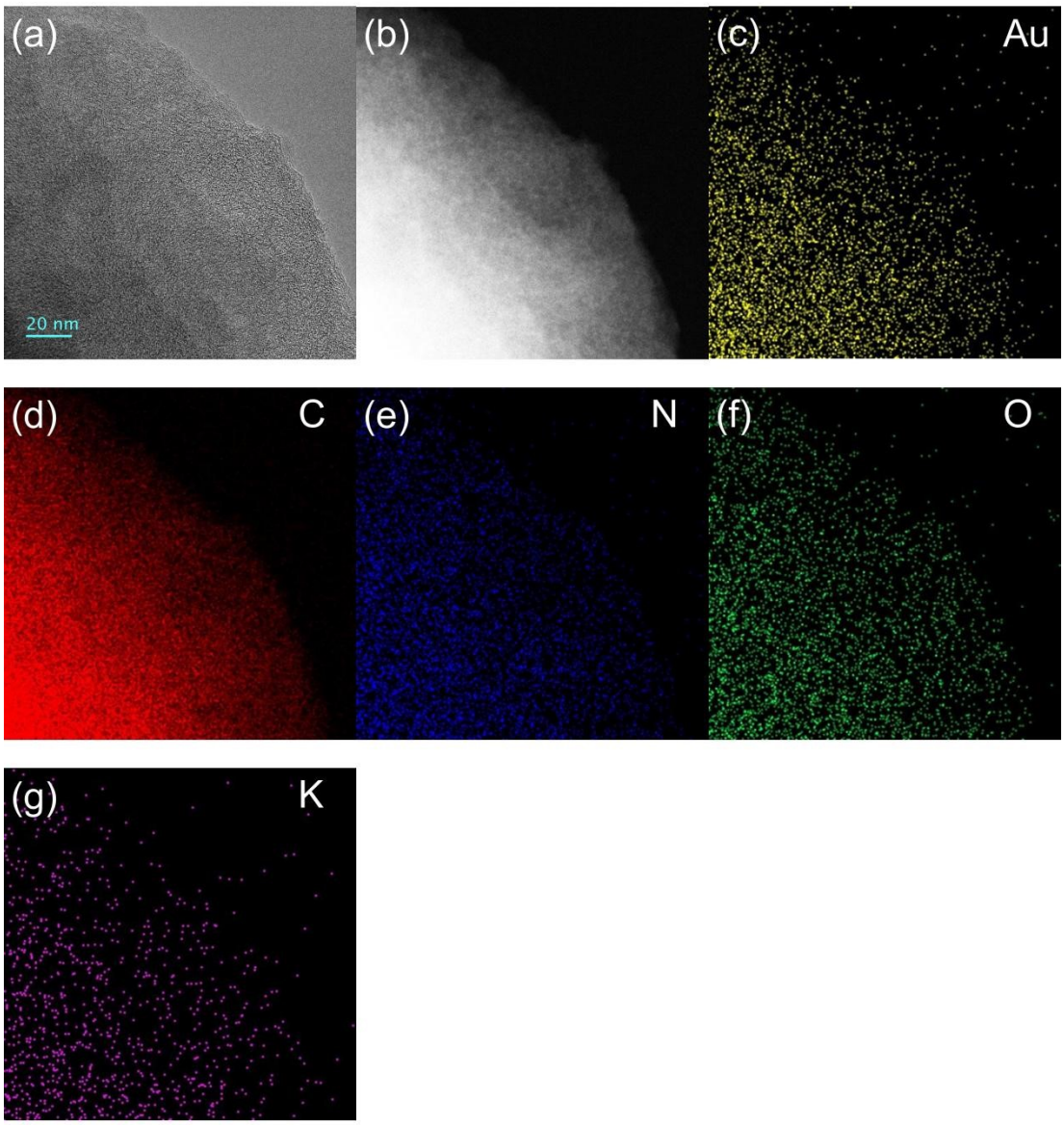

、**Figure S1.** (a) TEM image of Au/K-NC-SA; (b–g) Energy-dispersive X–ray spectroscopy (EDS) mappings of Au, C, N, O and K elements in Au/K-NC-SA.

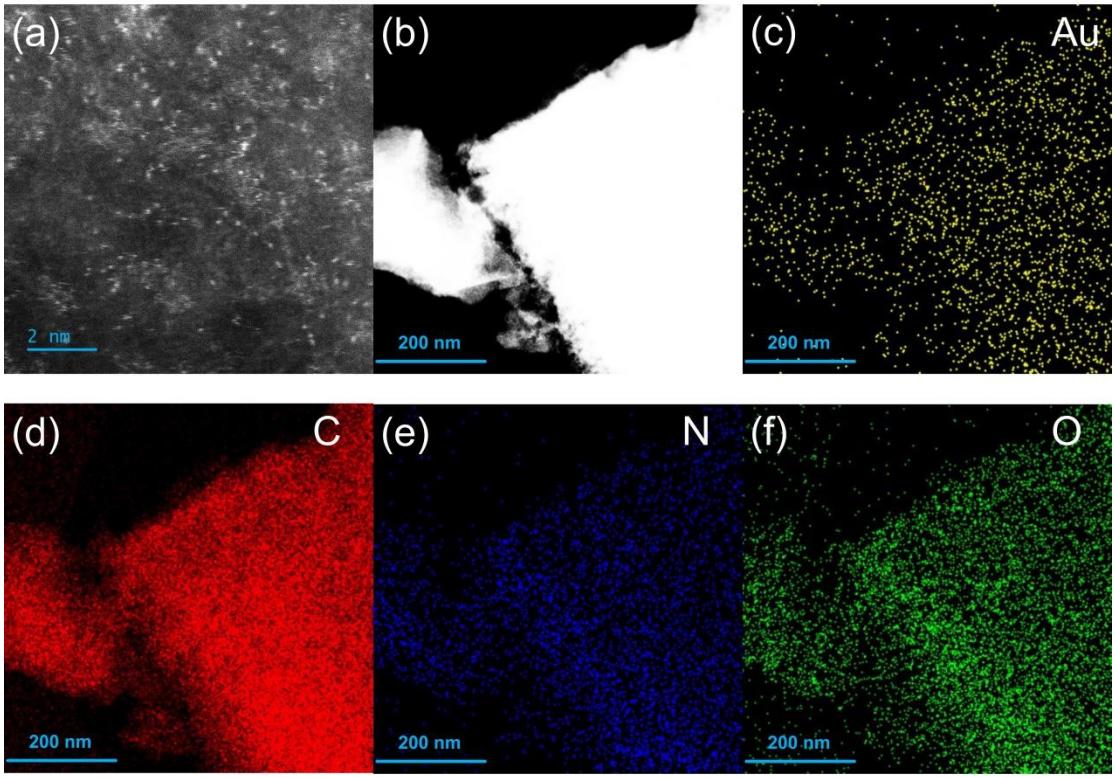

Figure S2. (a) TEM image of Au/NC-SA; (b–g) EDS mappings of Au, C, N and O elements in Au/NC-SA.

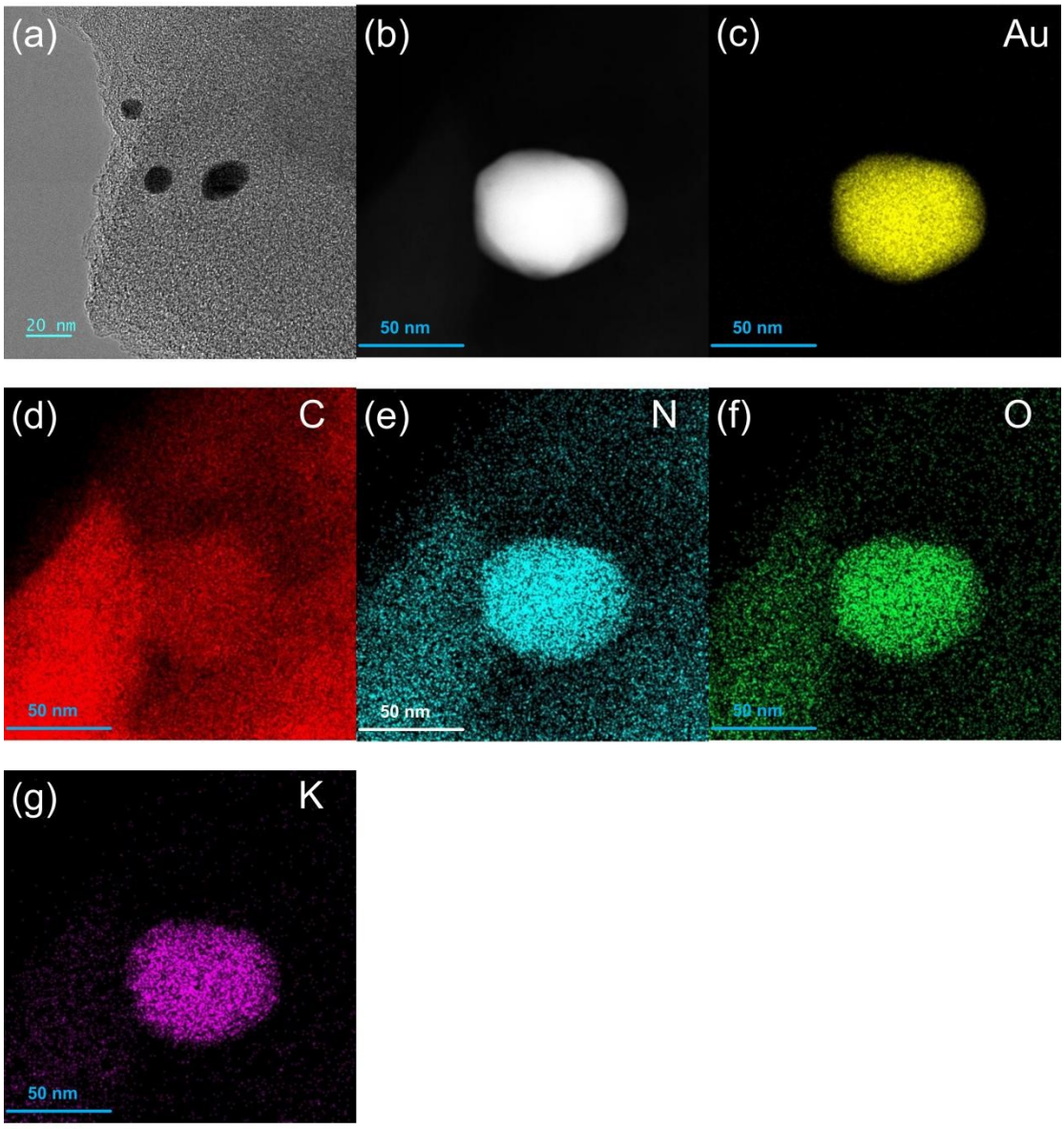

Figure S3. (a) TEM image of Au/K-NC; (b–g) EDS mappings of Au, C, N, O and K elements in Au/K-NC.

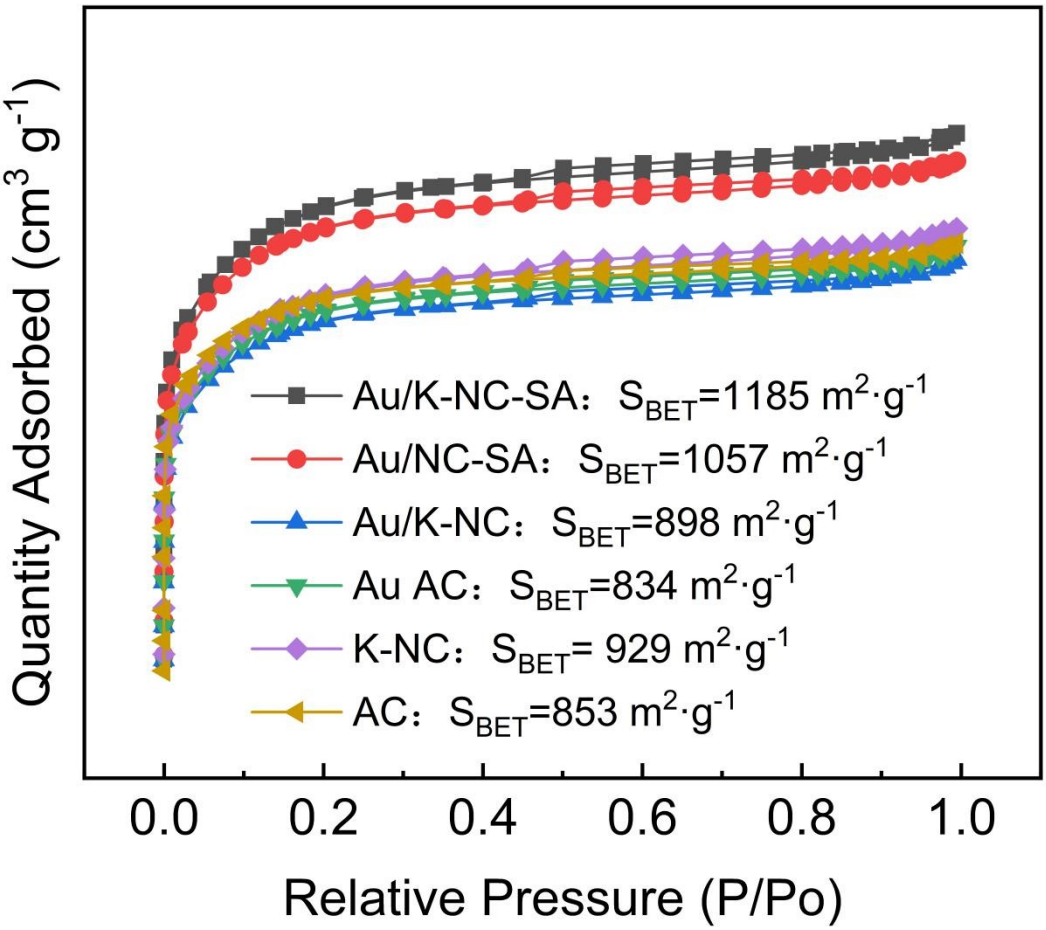

Figure S4. N_2 adsorption-desorption isotherms of post-reaction Au-based catalysts.

The post-reaction BET specific surface areas of various materials are simultaneously labeled in the figure. The specific surface area of Au/K-NC-SA (1057 $m^2 \cdot g^{-1}$) is slightly higher than that of Au/NC-SA and other materials.

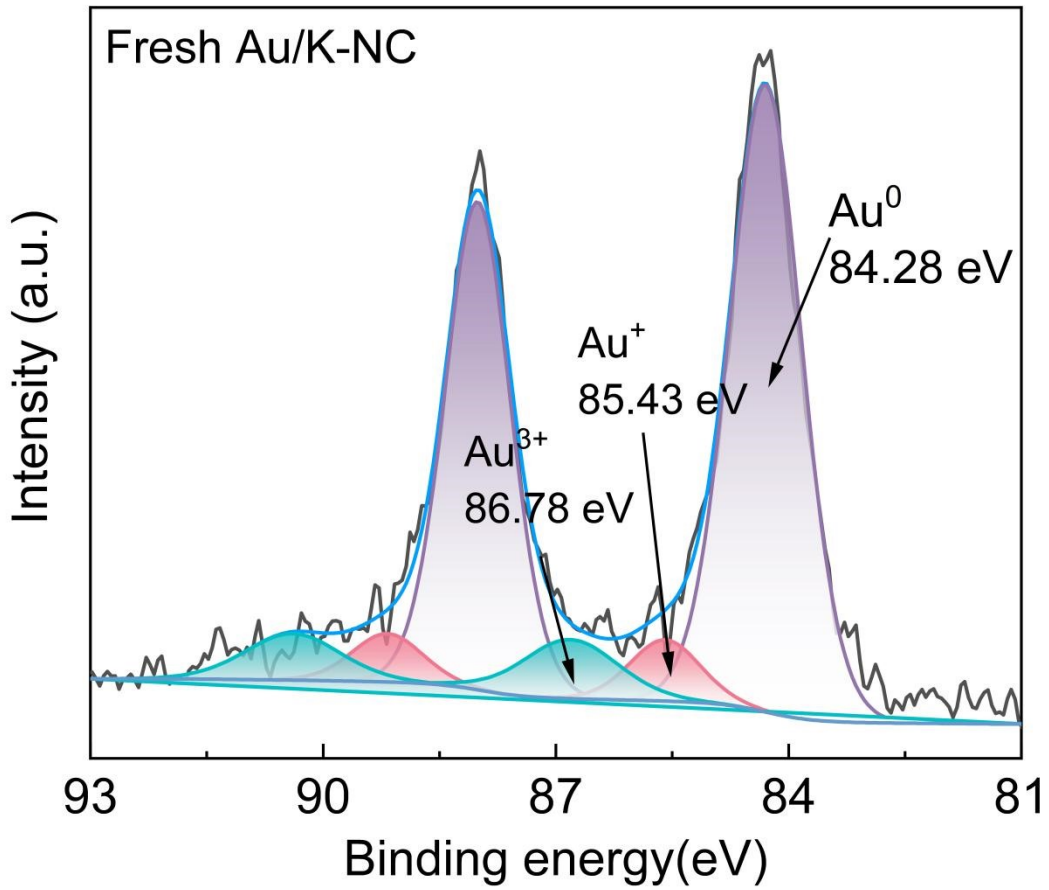

Figure S5. Au 4f XPS spectrum of Au/K-NC.

The Au 4f XPS spectra of Au/K-NC exhibit three binding energy peaks: at 84.28 eV corresponding to metallic Au^0, at 85.43 eV to Au^+, and one at 86.78 eV to oxidized Au^{3+}. Metallic Au^0 serves as the main component, accounting for 71.9% of the total Au content.

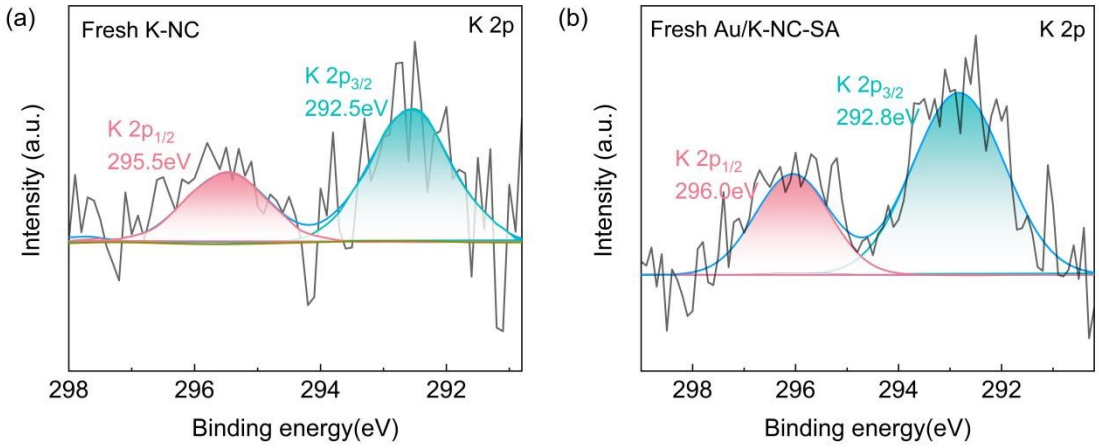

Figure S6. XPS K 2p spectra of K-NC and Au/K-NC-SA.

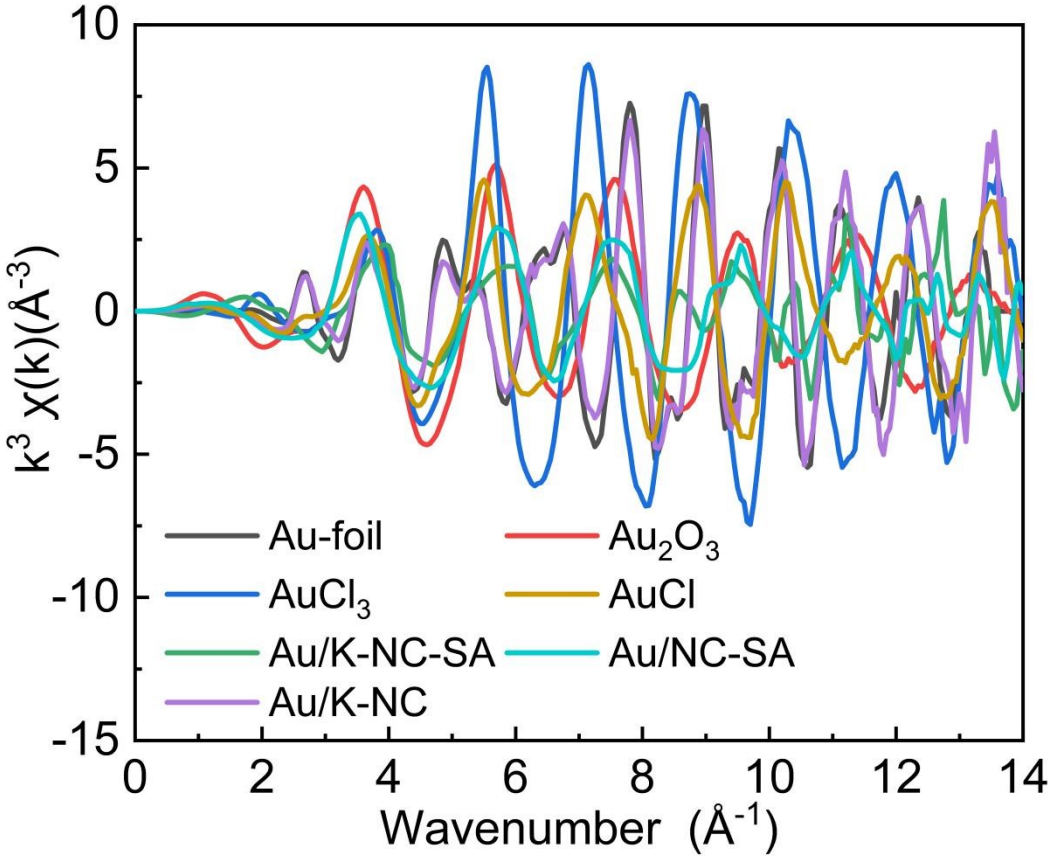

Figure S7. k^3–weighted k-space spectra of extended X–ray absorption fine structure (EXAFS) for Au/K-NC-SA, Au/NC-SA and Au/K-NC.

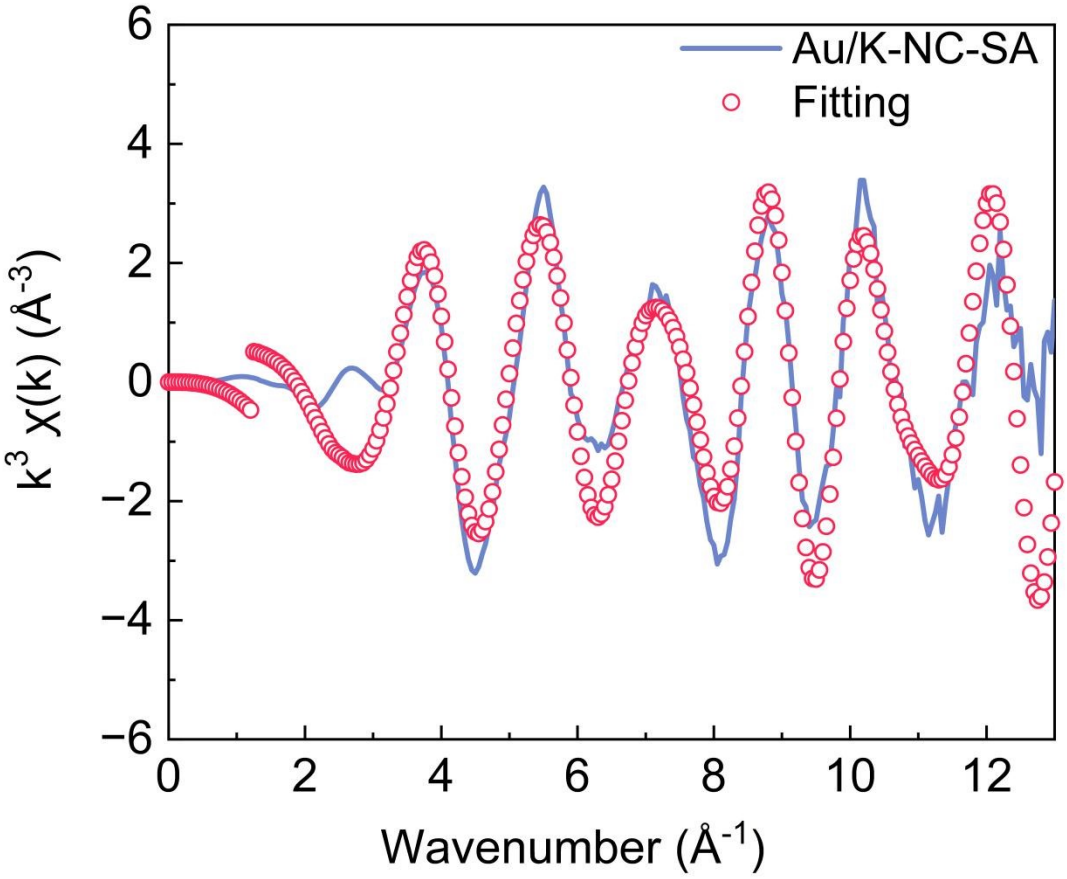

Figure S8. Analysis of Au/K-NC-SA by EXAFS at the Au L_3–edge in k-space.

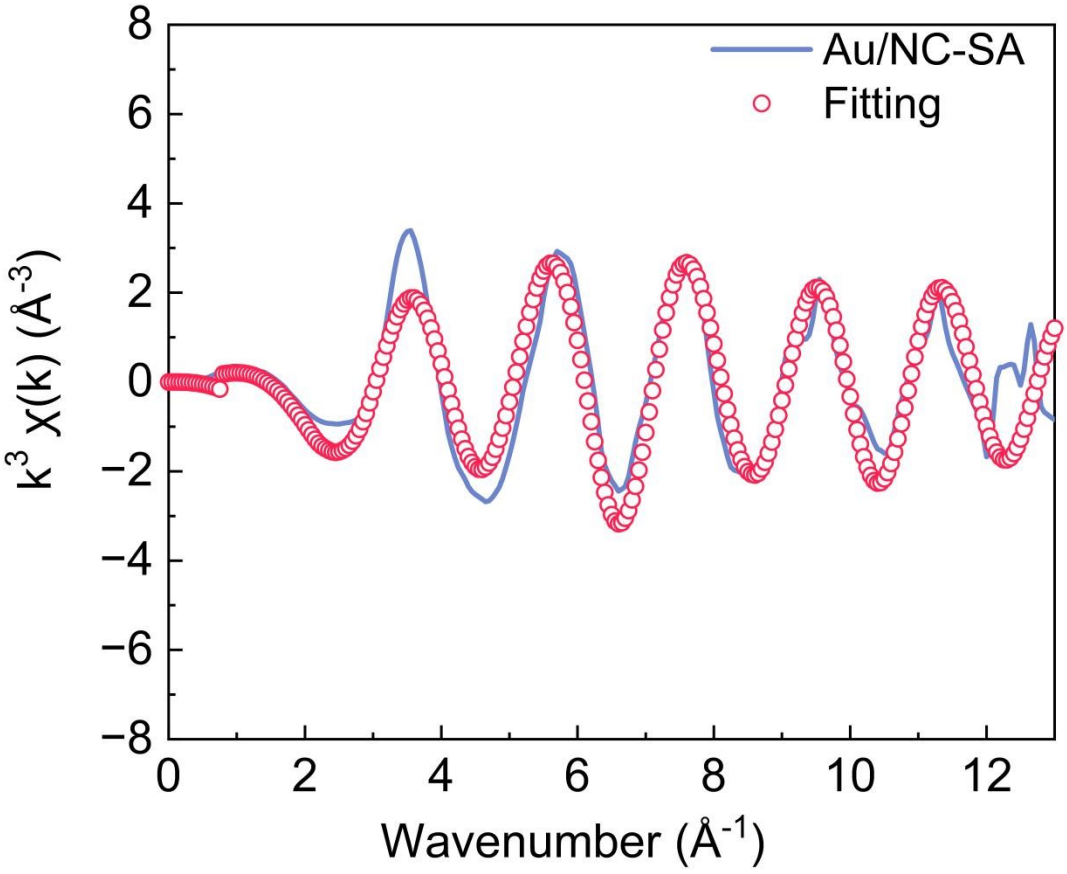

Figure S9. Analysis of Au/NC-SA by EXAFS at the Au L_3–edge in k-space

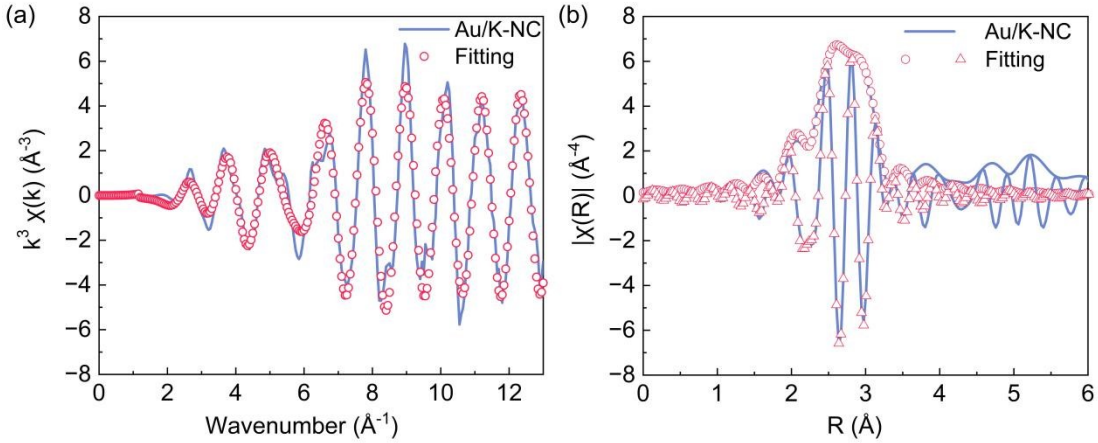

Figure S10. (a) k-space and (b) R-space EXAFS analysis of Au/K-NC at the Au L_3–edge.

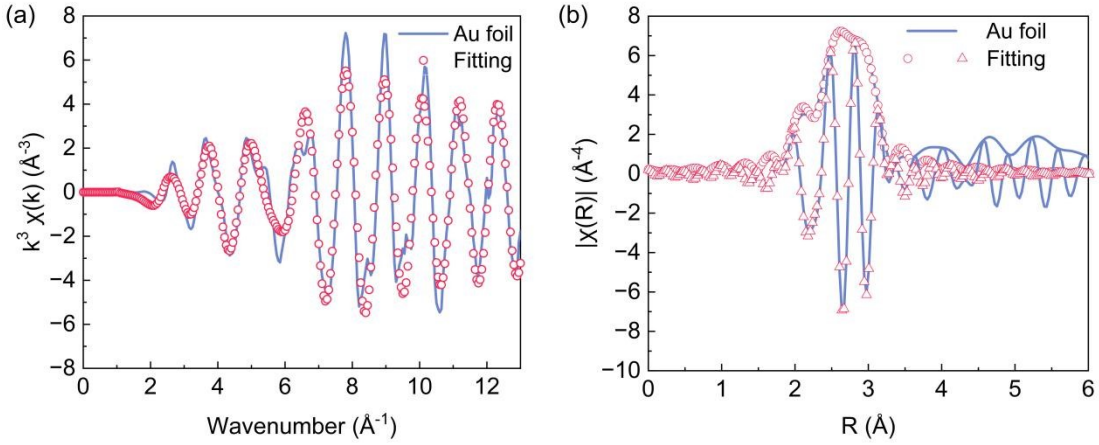

Figure S11. (a) k-space and (b) R-space EXAFS analysis of Au-foil at the Au L_3–edge.

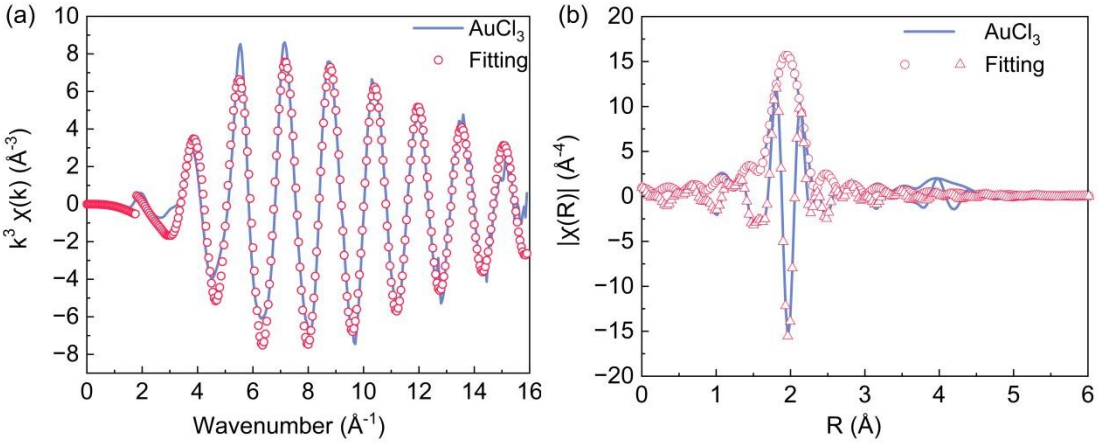

Figure S12. (a) k-space and (b) R-space EXAFS analysis of $AuCl_3$ at the Au L_3–edge.

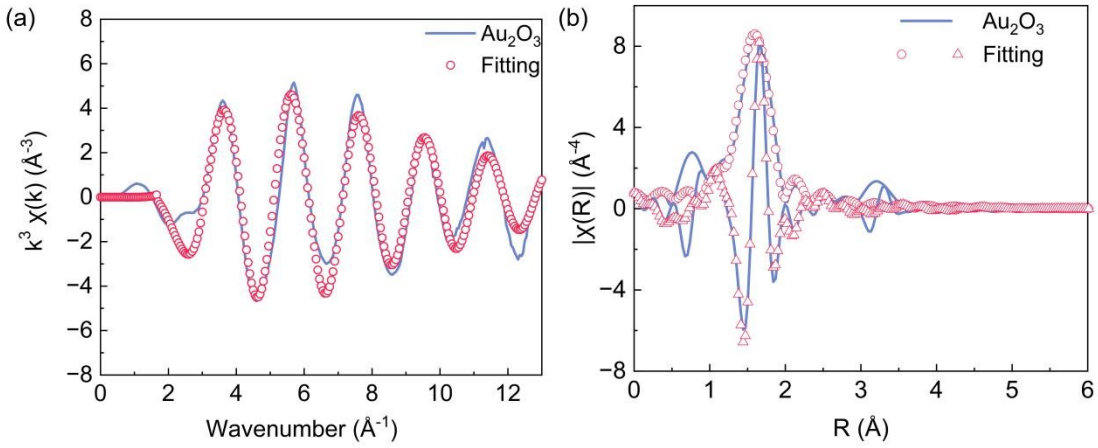

Figure S13. (a) k-space and (b) R-space EXAFS analysis of Au_2O_3 at the Au L_3–edge.

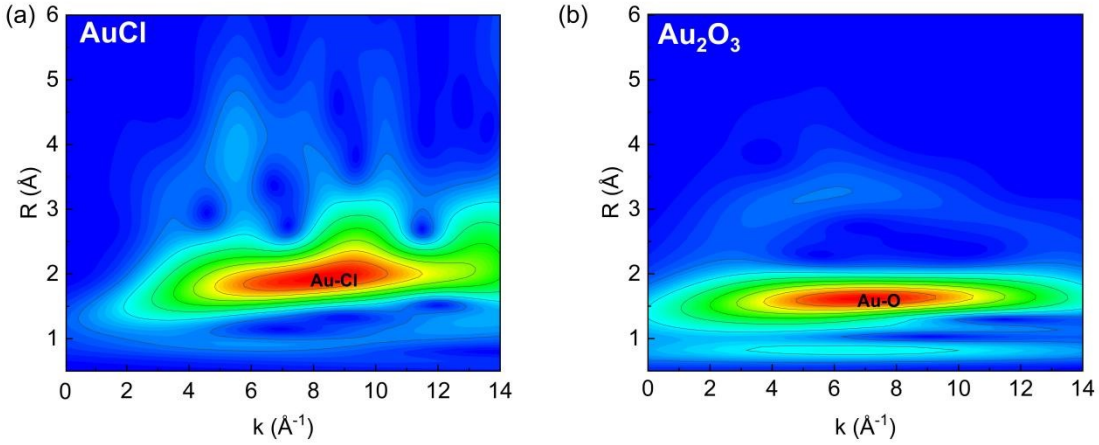

Figure S14. Wavelet transform was applied to the k^3–weighted EXAFS signals at the Au L_3–edge for (a) AuCl and (b) Au_2O_3.

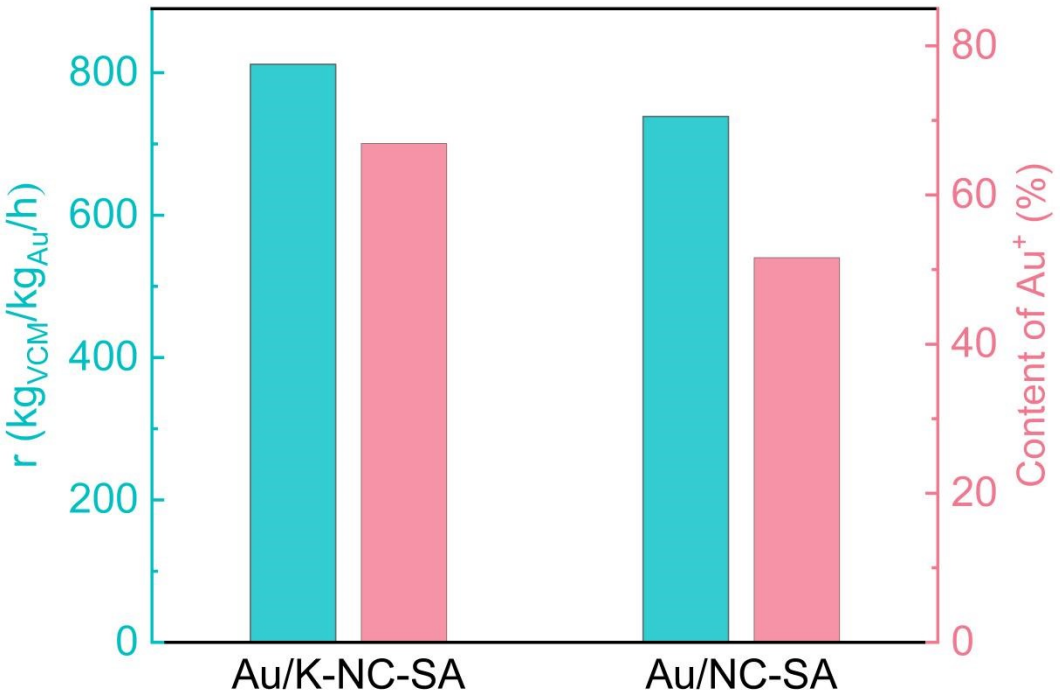

Figure S15. The correlation between the reaction rates of Au/K-NC-SA and Au/NC-SA and the content of Au^+ species.

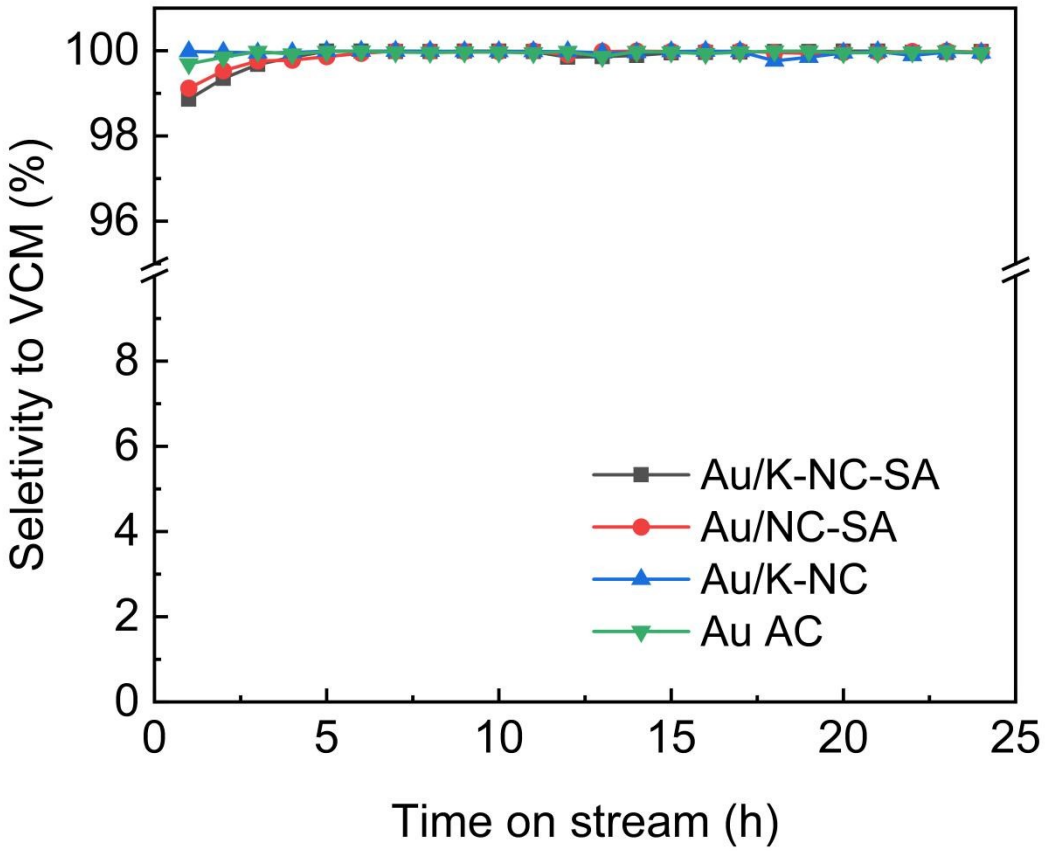

Figure S16. The selectivity to VCM over Au-based catalysts

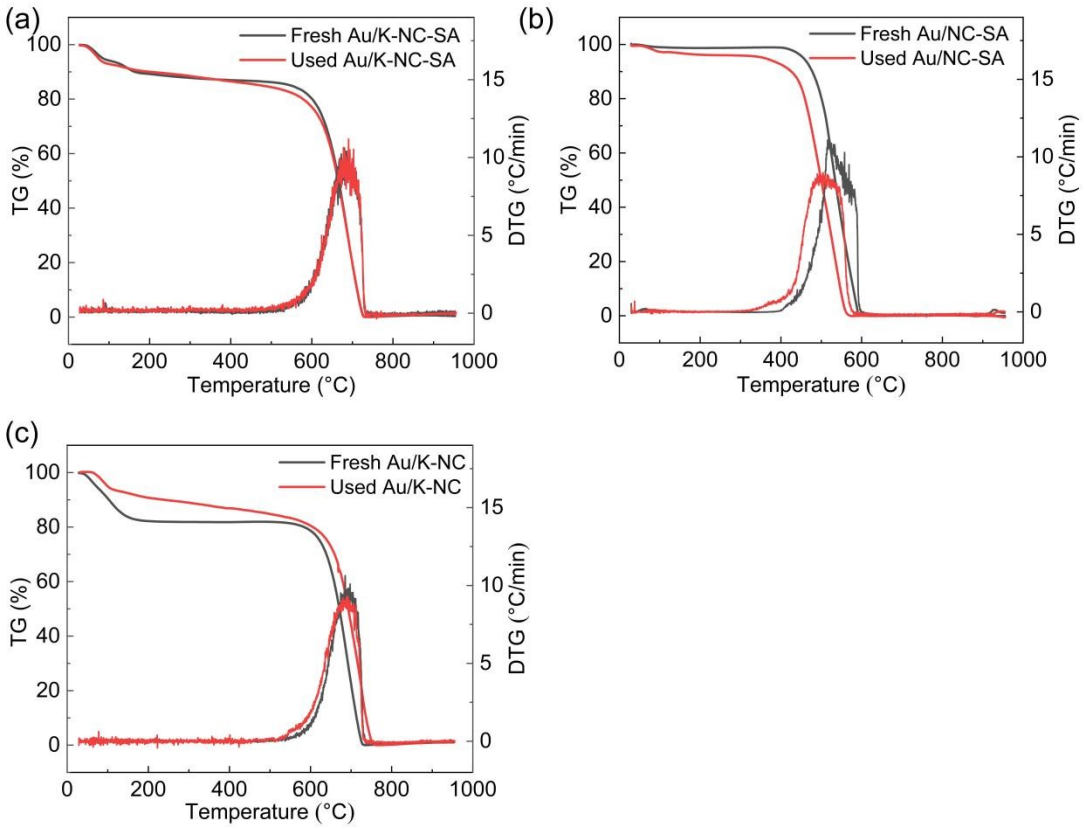

Figure S17. TG curve of Au/K-NC-SA,Au/NC-SA and Au/K-NC.

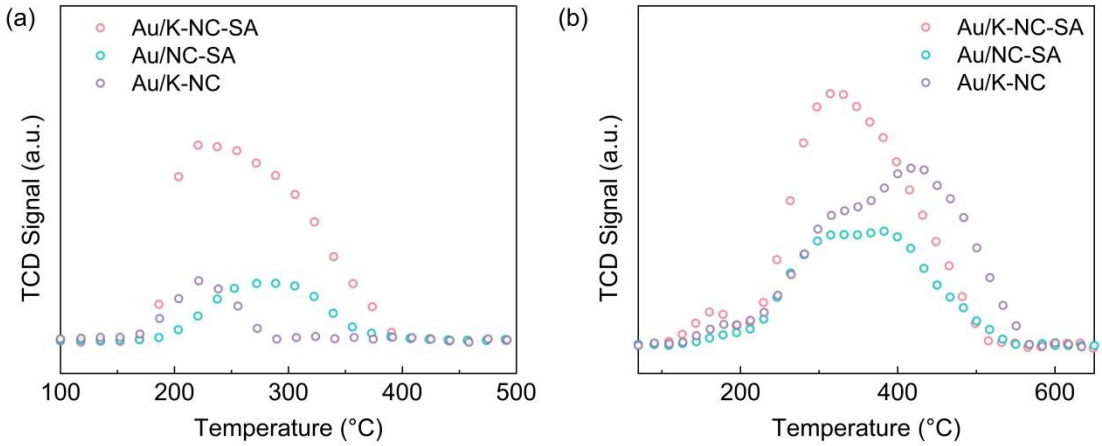

Figure S18. (a) HCl–TPD profiles of Au/K-NC-SA, Au/NC-SA and Au/K-NC; (b) C_2H_2–TPD profiles of Au/K-NC-SA, Au/NC-SA and Au/K-NC.

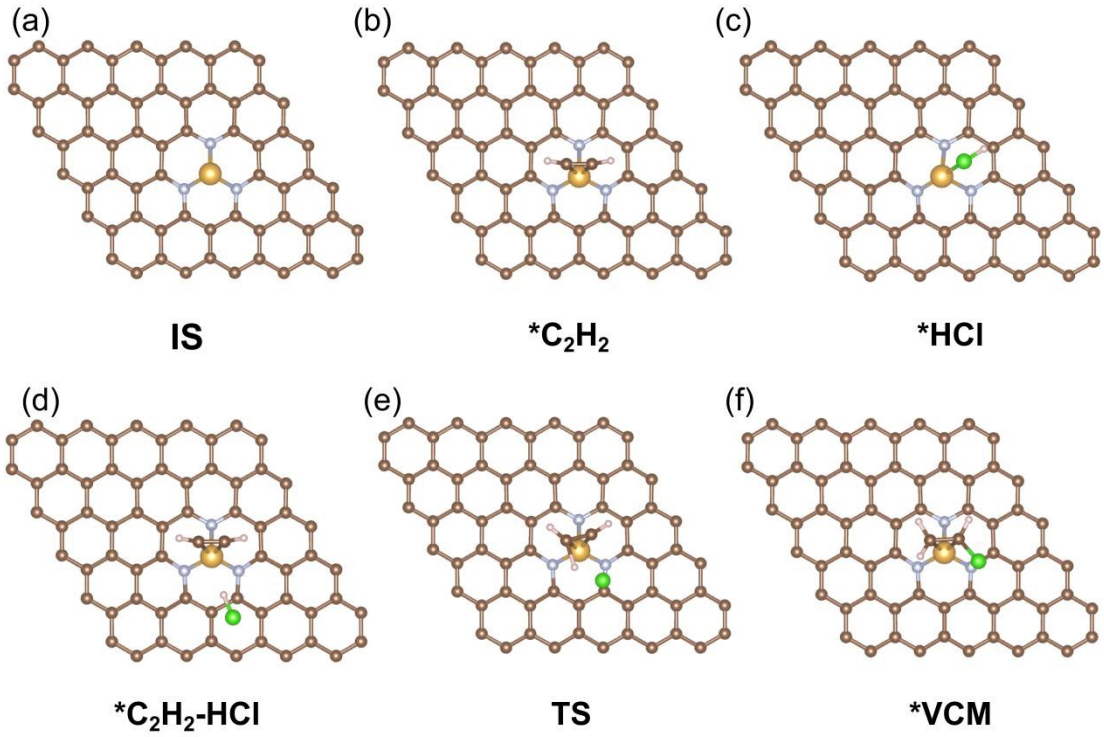

Figure S19. Configurations of species in the reaction pathway. (IS: Initial state of the Au/NC-SA catalyst; *: Adsorbed species including *C_2H_2, *HCl, reactant (*C_2H_2–HCl), and product (*VCM); TS: Transition state)

Table S1. The Au actual content of the samples deterimined by ICP–OES.

Samples	Au content (wt%)
Au/K-NC-SA	0.80
Au/NC-SA	0.81
Au/K-NC	0.82
Au AC	0.80

Table S2. The physical properties for all catalysts.

Samples	S_{BET} (m^2 g^{-1})	$\triangle S_{BET}$(%)	$S_{micro.}$ (m^2 g^{-1})	S_{micro}/S_{BET} (%)	$S_{ext.}$ (m^2 g^{-1})	S_{ext}/S_{BET} (%)	V_P (cm^3 g^{-1})	$\triangle V_P$(%)	$V_{micro.}$ (cm^3 g^{-1})	$V_{ext.}$ (cm^3 g^{-1})	D_{pore} (nm)
Fresh Au/K-NC-SA	1217	13.2	662	54.4	556	45.6	0.65	12.3	0.33	0.32	2.14
Used Au/K-NC-SA	1057		555	52.5	502	47.5	0.57		0.27	0.30	2.15
Fresh Au/NC-SA	1185	14.6	642	54.2	544	45.9	0.63	14.3	0.32	0.31	2.14
Used Au/NC-SA	1012		546	53.9	466	46.0	0.54		0.27	0.27	2.14
Fresh Au/K-NC	1062	23.5	548	51.6	515	48.4	0.58	24.1	0.27	0.31	2.17
Used Au/K-NC	812		437	53.8	375	46.2	0.44		0.22	0.22	2.18
Fresh Au AC	1095	23.8	562	51.3	533	48.7	0.59	22.0	0.28	0.31	2.17
Used Au AC	834		448	53.7	386	46.3	0.46		0.22	0.24	2.19
Fresh K-NC	1255	30.7	672	53.5	583	46.5	0.69	31.9	0.33	0.36	2.19
Used K-NC	870		440	50.6	430	49.4	0.47		0.22	0.25	2.17
Fresh AC	1285	33.6	676	52.6	609	47.4	0.69	33.3	0.33	0.34	2.19
Used AC	853		501	58.7	353	41.4	0.46		0.25	0.27	2.17

[a] S_{BET}: BET specific surface area; [b] t-plot micropore area; [c] t-plot external surface area; [d] V_P: total pore volume, volume at $p/p_0 = 0.98$; [e] t-plot micropore volume; [f] Adsorption average pore width (4V/A by BET).

Table S3. The contents and binding energy of different valence Au species in the Au catalysts.

Catalyst	Au species (%) (Binding energies (eV))		
	Au^0	Au^+	Au^{3+}
Au/K-NC-SA	/	73.2 (84.98 eV)	26.8 (86.73 eV)
Au/NC-SA	/	51.6 (85.13 eV)	48.4 (86.98 eV)
Au/K-NC	71.9 (84.28 eV)	12.2 (85.43 eV)	15.9 (86.78 eV)

Table S4. EXAFS fitting parameters at the Au L_3–edge for reference materials and samples。

Samples	Path	CN	R/Å	σ^2	ΔE_0	s_0^2	R factor
Au foil	Au–Au	12*	2.865±0.001	0.0086±0.0008	5.6±0.2	0.896±0.08	0.0057
Au_2O_3	Au–O	4*	1.981±0.004	0.0047±0.0006	10.7±0.5	0.95±0.04	0.0090
$AuCl_3$	Au–Cl	4*	2.287±0.001	0.0028±0.0001	11.7±0.1	0.86±0.01	0.0001
Au/K-NC-SA	Au–N	2.8±0.1	2.07±0.006	0.007±0.0003	13.2±2.1	0.896	0.04
Au/NC-SA	Au–N	3.3±0.1	2.02±0.005	0.002±0.0001	2.8±0.5	0.896	0.02
Au/K-NC	Au–Au	9.1±0.4	2.862±0.001	0.0073±0.0004	5.3±0.46	0.896	0.0037

(a) CN, coordination number; (b) R, distance between absorber and backscatter atoms; (c) σ^2, Debye-Waller factor to account for both thermal and stAuctural disorders; (d) ΔE_0, inner potential correction; R factor indicates the goodness of the fit. S_0^2 was fixed to 0.896, according to the experimental EXAFS fit of Au foil by fixing CN as the known cryst allographic value.

Table S5. TG-derived coke content of Au-based catalysts.

Samples	Amount of coke deposition (%)
Au/K-NC	6.30
Au/NC-SA	5.37
Au/K-NC-SA	3.18

Table S6. The deactivation rate of the catalyst

Samples	Inactivation rate (%/h)
Au AC	0.54
Au/K-NC	0.67
Au/NC-SA	0.08
Au/K-NC-SA	0.06

Table S7. Green index comparison of PVC industrial catalytic systems

Catalytic system	Atomic utilization (%)	Coke deposition amount (%)	Continuous operation time(h)	Environmental hazard	Industrial adaptability	Metal loading(wt%)	Ref
$HgCl_2$/AC	-	10-15	50-100	High (Hg pollution)	High (Existing process)	23.8	[14]
Cu/SAC	<30	10.6	50	Low	Low (Low activity)	15	[15]
Au/AC-D	<30	Relatively high	50-100	Low	Low (Lower stability)	1	[16]
Au/NC-SA	100	5.37	100	Low	Medium (Fast deactivation)	0.8	This work
Au/K-NC-SA	100	3.18	400	None	High (Existing process)	0.8	This work

Table S7 clearly demonstrates that our Au/K-NC-SA catalyst achieves 100% atomic utilization of Au, maintains 3.18% coke deposition, and enables 400 h of continuous operation—outperforming traditional $HgCl_2$/AC and literature Au/NC-SA systems in both environmental safety (no mercury pollution) and industrial adaptability, while reducing precious metal loading to 0.8 wt% for sustainable PVC production.

References

1. B. Ravel and M. Newville, *J. Synchrotron Radiat.*, 2005, **12**, 537-541.
2. S. Zabinsky, J. Rehr, A. Ankudinov, R. Albers and M. J. P. R. B. Eller, *Phys. Rev. B*, 1995, **52**, 2995.
3. H. Funke, A. Scheinost, M. J. P. R. B. C. M. Chukalina and M. *Physics*, 2005, **71**, 094110.
4. G. Kresse and J. J. P. R. B. Hafner, *Phys. Rev. B*, 1994, **49**, 14251.
5. G. Kresse and J. J. P. R. B. Hafner, *Phys. Rev. B*, 1993, **48**, 13115.
6. Y.-H. Wang, S. Zheng, W.-M. Yang, R.-Y. Zhou, Q.-F. He, P. Radjenovic, J.-C. Dong, S. Li, J. Zheng and Z.-L. J. N. Yang, *Nature*, 2021, **600**, 81-85.
7. J. P. Perdew, K. Burke and M. J. P. r. l. Ernzerhof, *Phys. Rev. Lett.*, 1996, **77**, 3865.
8. G. Kresse and J. J. C. m. s. Furthmüller, *Comput. Mater. Sci.*, 1996, **6**, 15-50.
9. G. Kresse and D. J. P. r. b. Joubert, *Phys. Rev. B*, 1999, **59**, 1758.
10. P. E. J. P. r. B. Blochl, *Phys. Rev. B*, 1994, **50**, 17953-17979.
11. S. Grimme, J. Antony, S. Ehrlich and H. J. T. J. o. c. p. Krieg, *J. Chem. Phys.*, 2010, **132**.
12. G. Henkelman, B. P. Uberuaga and H. J. T. J. o. c. p. Jónsson, *J. Chem. Phys.*, 2000, **113**, 9901-9904.
13. K. Niu, Z. Qi, Y. Li, H. Lin and L. J. T. J. o. P. C. C. Chi, *J. Phys. Chem. C*, 2019, **123**, 4969-4976.
14. S. Sun, H. Xu, Y. Fan, Z. Liu, Q. Hong, W. Huang, Z. Qu and N. Yan, *Ind. Eng. Chem. Res.*, 2022, **61**, 17057-17064.
15. Y. Wang, Y. Nian, J. Zhang, W. Li and Y. J. M. C. Han, *Mol. Catal.*, 2019, **479**, 110612.
16. G. Lan, Q. Ye, Y. Zhu, H. Tang, W. Han and Y. J. A. A. N. M. Li, *ACS Appl. Nano Mater.*, 2020, **3**, 3004-3010.